

PoPSAT (Polar Precipitation SATellite)



TEAM BLUE: Katrin Bentel, Matthias Binder, Even Birkeland, Clement Guilloteau, Eimante Kalinauskaite, Joshua Kiefer, Ana Lola Lopez, Michele Mione, Zoe Morland, Marco Palla, Georg Roth, Robert Ströbl, Cemal Melih Tanis, Maja Tomici, Victor Pellet
Team tutors: Luzius Kronig, Helmut Rott

Abstract: The terrestrial water cycle is a unique system on planet Earth. It is directly influenced by our changing climate with most drastic effects in the polar regions. A main element of the water cycle is precipitation, and it is only very sparsely observed at high latitudes. We propose a new satellite mission, POPSat, to observe snow and light rain at high latitudes, as well as snowfall at mid latitudes. The satellite will be equipped with a dual band (Ka and W bands) phased array antenna radar and provide 3D information about precipitation and clouds. The horizontal resolution of 2 km will exceed all other observations, and the measurements at high latitudes, together with the capability to monitor snowfall, will complement the GPM mission's observations. By filling this gap, POPSat will provide essential data for improving global weather and climate models.

1 Scientific background

Water, and the water cycle in particular, is surely fundamental to understand our Earth's functioning.

Precipitation is a key process in the weather and climate system, due to its storage, transport and release of latent heat in the atmosphere. In order to establish a global perspective of this process, observation from space is vital to produce globally consistent data, including areas unreachable by in-situ measurements. Precipitation has been extensively investigated in low latitudes, in which detailed models have been established for weather prediction. However, a gap has been left in higher latitudes above 65°, which prevents the creation of global un-

derstanding of precipitation's role in weather and climate [1].

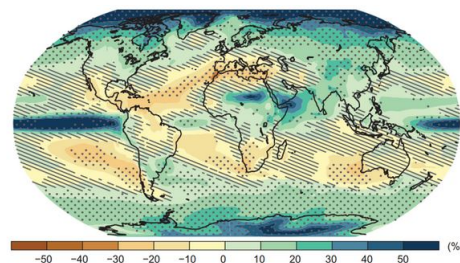


Figure 1: IPCC (2013): Climate Change 2013, The Physical Science Basis, Summary for Policymakers, 20

Present surface temperature observations and climate model simulations have estimated

that high latitudes show the strongest response to climate change in the world and that precipitation in high-latitudes will intensify into the future (see Figure 1). However, Climate models do not have the spatial resolution to represent the processes driving the precipitation in high latitudes (weather fronts, polar lows, convection, organised cold air outbreaks). Precipitation in Antarctica has not been accurately measured on a large scale due to the unique lower altitude rain and snowfall systems. This outlines the need for future observation to monitor the change in precipitation intensity and to provide precipitation properties for advancing and validating the parametrisation of precipitation processes in meteorological forecasting and climate modelling.

In doing this the gained knowledge has the potential of having a large impact on socioeconomics: more accurate and reliable weather prediction would influence high latitude inhabitants directly and help simplify the planning of polar shipping routes.

2 Scientific objective

Considering the current demand for data in order to predict the complex future of our climate, it is clear the focus of our mission should be to fill the gaps of current knowledge, specifically in unreachable areas that have limited observation. Therefore, our aim is to provide data to improve understanding of high latitude precipitation processes generating the following scientific objective:

SO1: Measure the precipitation rate in high latitudes at a scale compatible with mesoscale meteorological models.

Specifically, we will measure the contribution of 1) solid and liquid water particles, 2) stratiform and convective precipitation and 3) 3-D structure of precipitation systems to the climatology. As shown in figure 2, previous missions have been measuring precipitation properties, but only less than 65° N/S, which excludes the areas that are most indicative of the the extent of climate change. Moreover, Polar Prediction Project (World Weather Research Programme, World Climate Research Programme) outlines the requirement for verification and parameter-

isation of climate/weather models of key polar processes [2]. Therefore, measuring in high latitudes is our main purpose, because this is the current gap in knowledge.

SO2: Provide information of snowfall in lower latitudes to complement other missions

As Behrangi [1] points out, “Current orbital land precipitation products have serious shortcomings in detecting light rain and snowfall”. Since these resemble the most frequent types of global precipitation, we defined a second goal to provide additional data in order to gain understanding of snowfall at all latitudes.

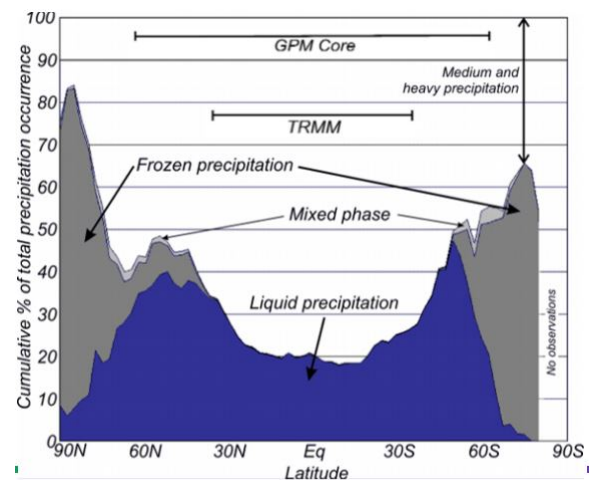


Figure 2: Mean zonal occurrence of oceanic light precipitation (as a percentage of total rainfall occurrence) derived from the Comprehensive Ocean-Atmosphere Data Set using ship-borne meteorological observations (1958-1991)[3]

2.1 Scientific requirements

SR1: Identification of solid and liquid water particles, with enough precision to determine their detailed distribution in Polar regions

To distinguish between different intensities of precipitation, it is required to detect liquid water within a specific dynamic range as well as the precision of measuring in different ranges of intensity (cf. Table 1). To target especially light to medium precipitation, which is expected to be the main type of precipitation in high latitudes (cf. Figure 2), the measurement range was adjusted according to this.

Parameter	Requirement	
	treshold	goal
Precipitation range	0.5 to 20	0.2 to 35
Precipitation rate accuracy		
≤ 2 mm/h	0.5 mm/h	0.2 mm/h
> 2 mm/h	20 %	10 %

Table 1: Radar Sensitivity & Accuracy Requirements

SR2: Horizontal Resolution 4 km (Threshold) /2 km (Goal) with a maximum deviance of 1/5 of the resolution

Our vertical resolution threshold is determined by weather models, which require a resolution of 4 km. This would observe mesoscale weather systems like fronts and polar lows in high latitudes that are usually several tens of kilometers in size.

However, smaller processes (convection, organised cold air outbreaks) with a scale of five kilometers require a finer resolution. Therefore, it is appropriate for our goal to have an increased resolution to a fraction of that (2km) to capture the most information of the system’s dynamics. The precision that has to be achieved is defined by the desired precision of geolocation, which must only deviate by 1 km in order to measure small- and mesoscale weather processes accurately.

SR3: Swath width of 150 km (Threshold)/ 300 km (goal)

Typical phenomena in high latitudes, such as polar lows, are normally a couple of hundred kilometres wide. Therefore, it is necessary to have a swath width of 150 km, to observe entire systems in one satellite passage. However, a width of 300 km would be very useful, as this range would ensure the observation of these phenomena.

SR4: Vertical Resolution of 1 km (Threshold)/ 200 m (Goal)

We know that the tropopause height at high latitudes is about 8 km, so it is necessary to measure at least 8-10 different points to have sufficient knowledge of what occurs at various altitudes in the troposphere. It would be better if we reach a resolution lower than 300m considering that troposphere has more or less 30

layers. Although, a resolution of 200m would allow us to have at least 1 point for every layer producing a very detailed vertical profile.

SR5: Vertical extent of scanning of 18 km

As said before, polar tropopause height is about 8 km in high latitudes. However, in order to exploit data from non polar regions, which can be useful to improve precipitation data globally, we have to consider the height of the tropopause at the equator, which is about 16 km. To ensure that the the troposphere at every latitude is included, it would be better to have a more extended region scanned: 18 km is surely a reassuring number.

SR6: Coverage of minimum 90% in latitudes higher than 50°

Especially the northern regions, due to their heterogeneous land masses, have mesoscale orographic driven weather systems, which deviate strongly from each other. 90% coverage in less than four days would be a good result for the mission, especially if the regions not observed are the two poles, as cyclones are expected to weaken the closer they are to the poles.

SR7: Mission duration of minimum 5 years

To reach the goal of gaining a better understanding of precipitation processes, it is vital to provide data for an appropriate timespan. The need of interannual comparison is caused by the high dependency of weather processes on seasonal variations, wherefore a minimum mission duration of 5 years is appropriate.

3 Instruments

3.1 Radar principles

The word radar is an acronym derived from the phrase RAdio Detection And Ranging and applies to electronic equipment designed for remotely detecting and tracking objects. Radar utilizes a technique known as the ‘Echo Principle’, meaning that extremely short bursts of radio energy are transmitted, reflected off a target and then returned as an echo. The antennas used for radar principles are either of the reflector type or of array type.

The standard scenario is reflection at a point

target or a surface. In the case of a weather radar, the signal is scattered and reflected by the droplets or snowflakes in precipitating clouds. This makes the standard radar principle slightly more complicated, which is elaborated in the following subsection.

3.2 Detecting precipitation with radar (measurement principle)

The following is an introduction to the principle of dual frequency measurements focusing on snowfall, the concept of which can be also suited for rainfall measurements.

Dual frequency radars offer enhanced detection of clouds, precipitation and snow. Expanding on the framework of the dual frequency radar on-board the Global Precipitation Measurement Satellite (GPM Core), which uses Ku/Ka dual band precipitation radar, we propose to use a dual frequency radar based on the two bands: Ka and W. The proposed instrument shall be used to retrieve precipitation comprising snowfall and low-to-medium intensity rainfall. W band is sensitive to snow particles. Dual frequency Ka/W band has been studied for modelling radar reflectivity for different models of snow particles, habits and diffusion[4][5]. Differential reflectivity in the two bands allows for the separation of the impact of different snow particle types on the scattering signal and supports the retrieval of snowfall rates. Figure 3 shows reflectivity measured in a single band. It can be seen that different particles with different shapes and different snowfall profiles can lead to the same reflectivity. The abscissa of the figure is a parameter of the snowfall profil, it is link to the snowfall rate via the parametric equation:

$$\lambda = 4100 S^{0.21} \quad (1)$$

where S is the snowfall.

As seen in Figure 4 differential reflectivity between Ka and W band is independent of the particle shape and thus is able to directly retrieve the snowfall parameters.

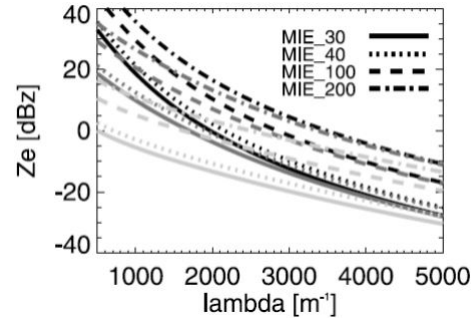


Figure 3: Effective reflectivity factor Z_e (dBz) as a function of the rainfall characteristic for the different snow particle models. The gray scale indicates the radar frequency: Ku , 13.4 GHz (black), Ka 36.5 GHz (dark gray) and W 89 GHz (light gray)

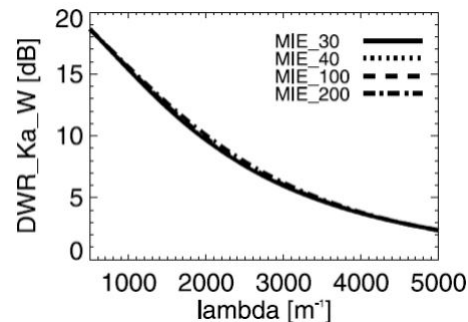


Figure 4: Dual wavelength ratio (DWR) in dB for 36.5 GHz (Ka band) and 94 GHz (W band) as a function of the distribution characteristic

3.3 Phased ray antenna

In contrast to a single dish, a phased array antenna consists of an array of individual antennas. Adding a phase shift to the signal received or transmitted by each antenna in an array of antennas allows the collective signal of these individual antennas to act as the signal of a single antenna. The radiation pattern can be reinforced in a given direction and electronically steered without moving mechanical elements, which enables switching the beam position as fast as the phase shifts. This is a major advantage for usage of array antennas over a single large antenna dish, which does it rather slowly. Furthermore, avoiding moving mechanical moving parts is a benefit for space applications.

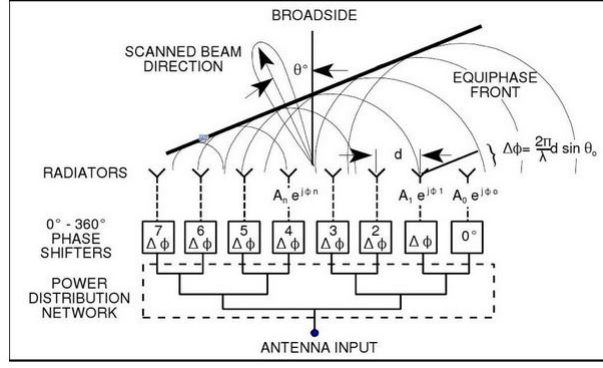


Figure 5: Phased array antenna block diagram

	Radar type	
	Ka-Band (36 GHz)	W-Band (94 GHz)
Scanning	cross-track scanning at nadir to 18°	cross-track scanning at nadir to 18°
Swath width	300 km	300 km
Resolution: range,spatial	500 m, 4 km (Nadir)	500 m, 2 km (Nadir)
Minimum detectable Ze & rainfall	10 dBz (0.2 mm/h)	-10 dBz (0.1 mm/h)
Measurement accuracy	1 dBz	1 dBz
Antenna dimensions	0.90 m x 0.90 m x 0.70 m	0.75 m x 0.75 m x 0.70 m
Mass	280 Kg	240 kg
Transmitted power: peak, mean	600 W, 8.6 W	1200 W, 17.2 W
Power consumption	300W	250W
Data volume	1.5 GB/day	1.5 GB/day

Table 2: Radar specifications

The proposed instrument is a uniform planar array which will consist of $N \times N$ array elements (see illustration of Figure 5) The first sidelobe level for such a distribution is typical of ~ -13 dB, meaning that ~ 99.9 % of the power is contained within the main beam.

Another advantage of a phased array antenna over a dish antenna in terms of reliability is that for a single antenna, if the positioning system fails, you can't point to anything except down the line of sight of the antenna. For the array antenna, if one antenna fails, all the rest continue to function and the collective pattern is modified slightly (called graceful degradation).

3.4 Instrument specification & final measurement product

The size of the Ka- and W- band phased array antennas is derived from the required half power

beamwidth. The radar equation

$$\bar{P}_r = \frac{P_t G_t G_r \lambda^2 V_c \bar{\eta}}{64\pi^3 R^4} \quad (2)$$

with

$$\bar{\eta} = \frac{\pi^5 |k|^2}{\lambda^4} Z \quad (3)$$

gives the relationship of power (P_r , P_t), gain (G_t , G_r), wavelength (λ) and range (R), and it also needs special terms for volume scattering, which is the case for observing precipitation. V gives the illuminated volume and the coefficient η relates to backscattering of unit volume. Z is the reflectivity coefficient which depends on the type, size and shape of the particles (section 3.2, Figure 3,4). mod K mod^2 is a factor defined by the permittivity of the reflecting particles (water or ice). These equations lead to our instrument specifications for the dual-band phased array radar instrument given in Table 2.

The final measurement product will be 3D precipitation information at 2 km horizontal and 500 m vertical resolution. It will also provide information about the type of precipitation and scattering from cloud particles.

4 Mission profile

4.1 Orbit

To fulfill the required mission objective of covering at least 90% of the polar region above 50° latitude, a Sun Synchronous Orbit (SSO) was chosen. The local time of descending node was chosen to be at 06:00 (LTDN 06:00). This is called a Dawn-Dusk Orbit. Apart from meeting the coverage requirement and providing a good mission operation from Europe, this kind of orbit is advantageous for the thermal subsystem. It ensures a consistent energy supply since the beta angle stays between 60 and 90 degrees. Eclipses occur only from May to August. To find a good relation between the orbit repeat cycle in days and the swath width (coverage), an optimization was performed. Resulting from the optimization the satellite has a designated swath width of 300 km (half cone angle $\sim 18^\circ$) with an altitude of 460 km. The orbit was not chosen higher since this would deduce a significant power increase of the instrument. On the other hand, a lower altitude causes a significantly higher atmospheric drag which, in turn, results in higher fuel consumption due to orbital control. After taking all aspects into account, the following orbit is chosen: LTDN 06:00 (Inclination $97,25^\circ$) with 460 km altitude.

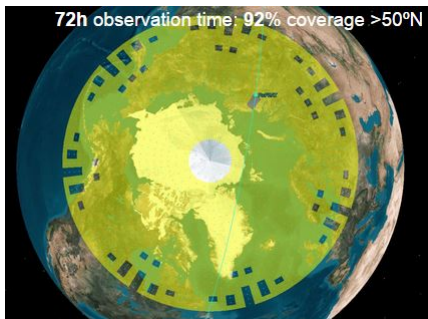


Figure 6: coverage of latitudes northward 50° after 3 days

This orbit enables a very good coverage with

a repeat cycle of 3 days. After 72 hours a coverage of 91.48% is achieved in the required region ($>50^\circ\text{N}$ latitude), as can be seen in the figure above.

4.2 Environment

Due to the low orbit there is no critical high radiation for the used components. Calculations with SPENVIS have shown that for a 5 year mission lifetime a total ionizing dose of 49.6 krad (incl. 100% margin) for an Aluminum shielding depth of 1mm and 7.0 krad (with 100% margin) for 2 mm of Aluminum are to expect.

5 Spacecraft

5.1 Spacecraft design

The spacecraft design is shown on Figure 7.

5.2 Structure & mechanism

The structural system of PoPSat builds on the cases of the two radar instruments. They are made from sandwich panels of aluminum honeycomb core and carbon-fibre-reinforced polymer facesheets for maximum stiffness while minimum weight. The same type of panels is used for the core structure of the satellite which accommodates the remaining subsystems, tanks, batteries, radiator, AOCS, etc., as well as for the solar panels. There are three solar panels of equal size, one of which forms the sun-pointing side of PoPSat, and two more unfolding from the same side of the satellite after launch through a spring-loaded hinge mechanism.

5.3 Attitude and orbital control system

The satellite is three-axis stabilized with the payload facing nadir. Through the used SSO we get an beta angle for the mission between 60° up to 85° which stays for the annual sun cycle on one side of the spacecraft. For the attitude and orbit determination the spacecraft uses sun sensors, magnetometer, star tracker, IMU and GPS. The critical components are available in a cold redundancy (e.g. star tracker, magnetometer. . .). Attitude control is provided with reaction wheels and magnetorquers.

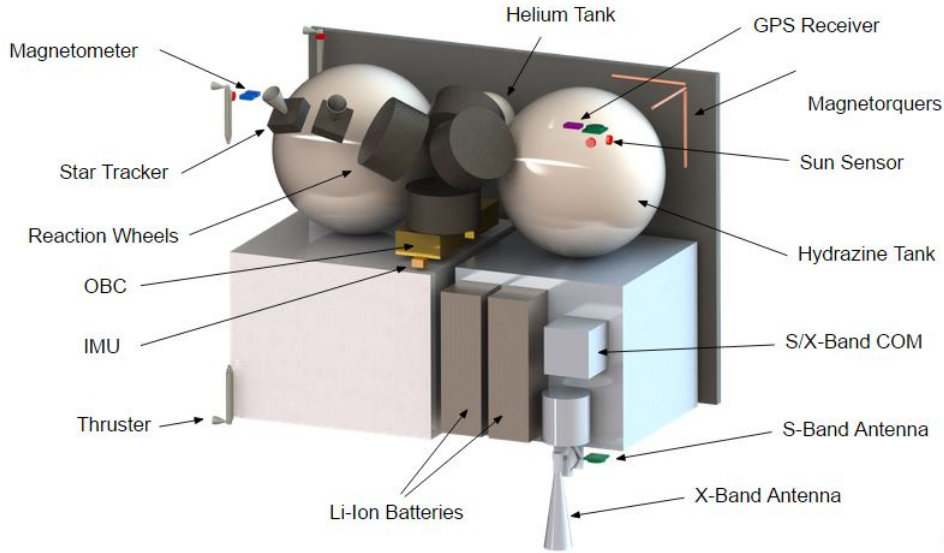


Figure 7: Payload desing

For dimensioning the components for the attitude control, we have considered the perturbations caused by gravity, drag, magnetic field and solar radiation. As it is a LEO, the main one is drag.

Component	Units	Characteristic
Reaction Wheels	4	Max torque:215Nm Max momentum:15Nms
Magnetorquer	3	Dipole moment:6 Am^2

Table 3: Attitude Control

5.4 Propulsion System

Due to the low altitude of 460 km, a propulsion system for orbital maintenance maneuvers is required. It will also be used for collision avoidance. Thus, a Hydrazine propulsion system with 4 thrusters will be deployed. Each thruster provides a thrust of 20 N and a specific impulse of 225 s. The thrusters have been all placed on the side which is opposite to the satellite's velocity vector. The necessary propellant is divided in two tanks of 135 l and there is also a high pressure helium tank.

5.5 Thermal Control System

The requirements for the thermal control system is to ensure a stable thermal environment

in the range of 25°C, to ensure that all components and subsystems are maintained within their required temperature limits. The three axis stabilized spacecraft in sun synchronous orbit leads to a simple model for external thermal loads.

Passive thermal control is accomplished by the use of appropriate thermal coatings on the spacecraft surface. The main body is insulated with a simple multilayer insulation blanket (MLI) of thin mylar sheets. The surface facing deep space is coated with aluminized kapton which has a high emissivity in IR and a relatively low absorptivity. This, along with placing the dissipating electronics on the emitting surface, prevents sunlight from excessively heating the satellite and allows heat to dissipate into space.

	Thermal models	
	Hot case	Cold case
Power dissipated	600W	300W
Solar flux	1420 W/ m^2	0 W/ m^2
Temperature with passive TC	49 °C	-33°C
Temperature with radiator, heater	~25°C	~25°C

Table 4: Results of the 1 knot thermal model of the satellite

Reasonable first order estimations of the spacecraft thermal control system is based on equilibrium temperature one node calculations for worst case hot and cold periods. This analysis lead to a worst case hot temperature of 48°C and cold temperature of -33°C in a passively cooled spacecraft. Thus, the spacecraft is equipped with a 1.6 m² Teflon radiator on the deep space facing surface for heat rejection and heaters to maintain operational or survival temperatures of all components during eclipse. Thermocouples should be installed to provide temperature data of various systems to the satellite's control system that then actuates heaters if necessary. Further analysis including a full thermal model of the spacecraft should be performed.

5.6 Power System

To provide the required energy for the instrument and all subsystem a power source and storage system has to be deployed. Since the spacecraft operates in LEO at approximately 1 AU, the solar flux is sufficiently high to use solar arrays. However, to reduce the atmospheric drag which will be experienced by the satellite at this low altitude, small arrays are required. Thus, triple-junction Gallium Arsenide (GaAs) cells which achieve an efficiency of about 30% have been chosen to provide the spacecraft with energy. For the calculation of the array size a maximum eclipse time of 23.8 min was considered. Moreover, an inherent degradation of 0.77 and a worst case incident angle of 30° are expected. The annual degradation is assumed to be 3.75%. This yields a total solar array size of 8.3 m² which will be subdivided into three panels. The distribution of the energy to all subsystems will be achieved by a 28 V regulated bus.

Since the instrument and the subsystems of the satellite have to work during eclipse time, an energy storage system has to be installed. Thus, to guarantee redundancy, two Lithium-ion batteries will be used. In total, they provide a capacity of 965 Wh. This includes a transmis-

sion efficiency of 90% and a Depth-of-Discharge of 50%. This ensures the batteries to provide enough energy over the entire mission lifetime.

5.7 Onboard Computer (OBC) & Data Handling

For the onboard computing a COTS OBC gets used, two OBC in cold redundancy. The onboard computer handles the control functions of the satellite (power, thermal,payload), in addition it handles the AOCS control algorithm, the housekeeping data, telemetry data.

5.8 Ground Segment and Data Link

For polar orbiting satellites, a single high latitude ground station can provide good coverage. Using the KIR-2 13 m antenna at Kiruna Es-track ground station in northern Sweden will give 7-8 access windows per day to a satellite in 460 km solar synchronous orbit with a mean duration of 315 second. The Kiruna ground station can provide tracking, telemetry, telecommand and radiometric measurements in the S-band, and downlink in the X-band of up to 100 Mb/s.

5.9 Telemetry, Tracking & Commanding (TT&C)

The TT&C process consists of downloading information about the satellites position, attitude and system health, and uploading commands such as antenna pointing and orbital adjustments. The TT&C has a low data volume, but it is crucial that it a link is functional regardless of the satellites attitude since the satellite is useless if it can't be communicated with. To ensure communication with any satellite attitude, two patch antennas facing opposite ways so that their radiation patterns overlap. A relatively small bandwidth of 8 kb/s up and 4 kb/s will provide a good signal to noise ratio even when the signal is weak, and using a modulation scheme that only requires a 3 dB signal to noise ratio (BPSK w/Viterbi) we can be confident that we will always be able to communicate with the satellite.

	S up (4 kb/s)	S down (8 kb/s)	X down (100 Mb/s)	Unit
EIRP	69.0	0	21	dBW
Transmission loss	-169	-169	-180	dB
G/T	-38	21	36	dB/K
Eb/N0	43	30	26	dB
Required Eb/N0	3	3	10	dB
Margin	40	27	17	dB

Table 5: Link budgets for S-band up/downlink and X-band downlink

To ensure communication with any satellite attitude, two patch antennas facing opposite ways so that their radiation patterns overlap. A relatively small bandwidth of 8 kb/s up and 4 kb/s will provide a good signal to noise ratio even when the signal is weak, and using a modulation scheme that only requires a 3 dB signal to noise ratio (BPSK w/Viterbi) we can be confident that we will always be able to communicate with the satellite.

5.10 Downlink

With two instruments gathering data at a rate of 140 kb/s each, a total of 3 GB of data will be produced daily. With an X-band link of 100 Mb/s this can be done in 242 seconds which leaves a 30% margin for the mean access duration.

In order to take advantage of the 100 Mb/s downlink a modulation scheme such as QPSK is needed. This requires a signal to noise ratio of 9.6 dB to have a bit error rate under 10^{-6} which will be achieved by using a 15 dB horn antenna mounted to an antenna pointing mechanism.

5.11 Link budgets

From the link budgets we can see that we can achieve our communication goal with a large margin (see Table 5)

5.12 Satellite budgets

The preliminary mass and power breakdown for the PoPSAT are briefly reported in table 5.

A margin of 10% was applied to all subsystems' masses, while a margin of 50% was applied to the payload mass. Moreover, a system level margin of 20% was applied to the overall mass. The payload mass accounts for the 40% of the

satellite dry mass. Regarding the power, the PoPSAT payload consists of a dual-frequency radar instrumentation which requires a power of ~ 600 W, including a 10% margin. This drives the power breakdown of the the entire satellite and allows to estimate the power required from each subsystem. A 10% system level margin was applied to the overall satellite power.

5.13 ΔV budget

Manoeuvre	Total ΔV with margins (m/s)
Launcher dispersion	36.6
Stationkeeping	184.4
Safe mode reserve	35.3
Collision avoidance	10.5
Total	267.3

Table 6: Link budgets for S-band up/downlink and X-band downlink

6 Launcher

With a mass of 2398 kg (with margins) and size of 1,7 x 1 x 1,4 m (stowed) the satellite fits into the mass and dimension envelope of the fairing of a Soyuz Fregat-2B. The spacecraft fits into the lower or in the top compartment which allows a dual launch with a second satellite. This drastically reduces the launch costs. The performance of the Soyuz allows to bring a total weight of 4500 kg into a SSO. The spacecraft fits in the lower or in the top compartment, thus makes dual launch with a second satellite possible. Which can cause a reduction of the launch costs.

	component	mass with margin (kg)	power with margin (W)
	Payload	780	605
s	AOCS	46	105
u	TTC,antennas	12	50
b	OBC	94	50
s	Power battery		
y	earness	250	78
s	Structure &		
t	Mechanism	383	10
e	Thermal	38	52
m	Propulsion	39	80
Launch veichle adapter		116	-
Propellant		241	-
Total		1999	1057
Total with 20% SLM		2398	1163

Table 7: PoPSAT mass and power budget

The performance of the Soyuz allows to bring a total weight of 4500 kg into an SS Orbit.

7 Cost & risk assesment

In the following table are summarized PoPSAT costs:

item	M €
Project team	35
Industrial costs	178
Mission operations	40
Science operations	25
Payload	175
Launcher (Soyuz) shared	40
Contingency	68
Total	561

Table 8: Estimated costs for PoPSAT with a mission lifetime of 5 years

The highest risk follows from the development of the W-Band phased array antenna. A low overall risk for the improvement of the Ka-Band is given through the availability of space qualified systems, this results in an overall risk of 4 (minimum and acceptable). For the development of the W-Band phase array antenna a overall risk of 6 was estimated which means a low and acceptable.

8 Conclusions

PoPSAT will be the first mission to provide high resolution 3-D structure of precipitation systems in high latitudes and observe snowfall, light precipitation, and cloud structure across all latitudes. It will provide precipitation properties for advancing and validating the parameterisation of precipitation processes in meteorological forecasting and climate modelling.

References

- [1]National Aeronautics and Space Administration & Japanese Aerospace Exploration Agency, (2014), Global Precipitation Measurement Press Kit, p.4 (Quick Facts)
- [2]Polar Prediction (2012): Goals, URL: <http://www.polarprediction.net/about-ppp/goals/> (18.07.2016)
- [3]EGPM (2004): SP-1279 (5), 10
- [4]Kulie, M. S., M. J. Hiley, R. Bennartz, S. Kneifel ,and S. Tanelli, 2014: Triple frequency radar reflectivity signatures of snow: Observations and comparisons to theoretical ice particle scattering models. *J. Appl. Meteor. Clim.*, 53, 1080-1098.
- [5]Kneifel, S., M. S. Kulie, and R. Bennartz, 2011: A triple-frequency approach to retrieve microphysical snowfall parameters. *J. Geophys. Res.*, 116, D11203, doi:10.1029/2010JD015430.